PROCEEDINGS OF SCIENCE

MLMC: Machine Learning Monte Carlo for Lattice Gauge Theory

PoS(LATTICE2023)036

Sam Foreman,[a,*] **Xiao-Yong Jin**[a,b] **and James C. Osborn**[a,b]

[a] *Leadership Computing Facility, Argonne National Laboratory, 9700 S. Cass Ave, Lemont IL, USA*

[b] *Computational Science Division, Argonne National Laboratory, 9700 S. Cass Ave, Lemont IL, USA*

E-mail: foremans@anl.gov, xjin@anl.gov, osborn@alcf.anl.gov

We present a trainable framework for efficiently generating gauge configurations, and discuss ongoing work in this direction. In particular, we consider the problem of sampling configurations from a 4D $SU(3)$ lattice gauge theory, and consider a generalized leapfrog integrator in the molecular dynamics update that can be trained to improve sampling efficiency. Code is available online at l2hmc-qcd.

The 40th International Symposium on Lattice Field Theory (Lattice 2023)
July 31st - August 4th, 2023
Fermi National Accelerator Laboratory

*Speaker

1. Introduction

We would like to calculate observables O:

$$\langle O \rangle \propto \int [\mathcal{D}x]\; O(x)\, \pi(x) \tag{1}$$

where $\pi(x) \propto e^{-\beta S(x)}$ is our target distribution. If these were independent, we could approximate the integral as $\langle O \rangle \simeq \frac{1}{N}\sum_{n=1}^{N} O(x_n)$ with variance

$$\sigma_O^2 = \frac{1}{N}\mathrm{Var}\left[O(x)\right] \Longrightarrow \sigma_O \propto \frac{1}{\sqrt{N}}. \tag{2}$$

Instead, nearby configurations are correlated, causing us to incur a factor of τ_{int}^{O} in the variance expression

$$\sigma_O^2 = \frac{\tau_{\mathrm{int}}^{O}}{N}\mathrm{Var}\left[O(x)\right]. \tag{3}$$

1.1 Hamiltonian Monte Carlo (HMC)

The typical approach [8, 9] is to use Hamiltonian Monte Carlo (HMC) algorithm for generating configurations distributed according to our target distribution $\pi(x)$. This can be done by sequentially constructing a chain of states $\{x_0, x_1, x_2, \ldots, x_i, \ldots, x_n\}$, such that, as $n \to \infty$:

$$\{x_i, x_{i+1}, x_{i+2}, \ldots, x_n\} \sim \pi(x). \tag{4}$$

Figure 1: Leapfrog update.

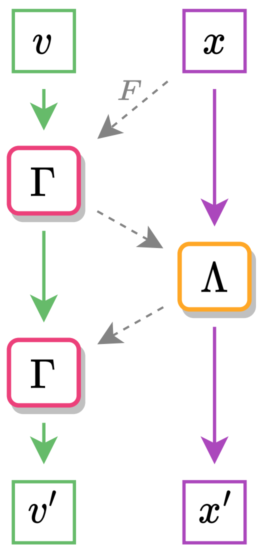

To do this, we begin by introducing a fictitious momentum[1] $v \sim \mathcal{N}(0,1)$ normally distributed, independent of x. We can write the joint distribution $\pi(x, v)$ as

$$\pi(x, v) = \pi(x)\pi(v) \propto e^{-S(x)} e^{-\frac{1}{2}v^T v} \tag{5}$$

$$= e^{-\left[S(x) + \frac{1}{2}v^T v\right]} \tag{6}$$

We can evolve the Hamiltonian dynamics of the $(\dot{x}, \dot{v}) = (\partial_v H, -\partial_x H)$ system using operators $\Gamma : v \to v'$ and $\Lambda : x \to x'$. Explicitly, for a single update step of the leapfrog integrator:

$$\tilde{v} := \Gamma(x, v) = v - \frac{\varepsilon}{2}F(x) \tag{7}$$

$$x' := \Lambda(x, \tilde{v}) = x + \varepsilon\tilde{v} \tag{8}$$

$$v' := \Lambda(x', \tilde{v}) = \tilde{v} - \frac{\varepsilon}{2}F(x'), \tag{9}$$

where we've written the force term as $F(x) = \partial_x S(x)$. Typically, we build a trajectory of N_{LF} leapfrog steps $(x_0, v_0) \to (x_1, v_1) \to \cdots \to (x', v')$, and propose x' as the next state in our chain. This proposal state is then accepted according to the Metropolis-Hastings criteria [25]

$$A(x'|x) = \min\left\{1, \frac{\pi(x')}{\pi(x)}\left|\frac{\partial x'}{\partial x}\right|\right\}. \tag{10}$$

[1] Here $\sim$ means *is distributed according to*.

2. Method

Unfortunately, HMC is known to suffer from long auto-correlations and often struggles with multi-modal target densities. To combat this, we propose building on the approach from [8–10]. We introduce two (invertible) neural networks `xNet` : $(x, v) \to (\alpha_x, \beta_x, \gamma_x)$, `vNet` : $(x, F) \to (\alpha_v, \beta_v, \gamma_v)$. Here, (α, β, γ) are all of the same dimensionality as x and v, and are parameterized by a set of weights θ. These network outputs (α, β, γ) are then used in a generalized MD update (as shown in Fig 2) via:

$$\boxed{\Gamma_\theta^\pm} : (x, v) \to (x, v'), \tag{11}$$

$$\boxed{\Lambda_\theta^\pm} : (x, v) \to (x', v). \tag{12}$$

where the superscript $\pm$ on $\Gamma_\theta^\pm$, $\Lambda_\theta^\pm$ correspond to the direction $d \sim \mathcal{U}(-1, +1)$ of the update.
To ensure that our proposed update remains reversible, we split the x update into two sub-updates on complementary subsets ($x = x_A \cup x_B$):

Figure 2: Generalized MD update.

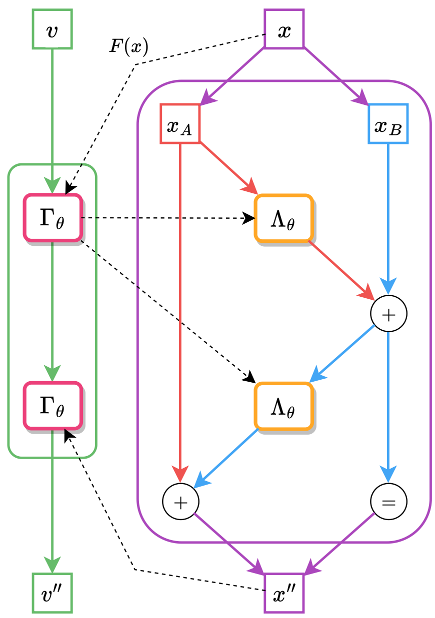

$$v' = \Gamma_\theta^\pm(x, v) \tag{13}$$

$$x' = x_B + \Lambda_\theta^\pm(x_A, v') \tag{14}$$

$$x'' = x'_A + \Lambda_\theta^\pm(x'_B, v') \tag{15}$$

$$v'' = \Gamma_\theta^\pm(x'', v') \tag{16}$$

2.1 Algorithm

1. `input:` x
   - Re-sample $v \sim \mathcal{N}(0, 1)$
   - Construct initial state $\xi := (x, v)$
2. `forward:` Generate proposal ξ' by passing initial ξ through N_{LF} leapfrog layers:

$$\xi \xrightarrow{\text{LF Layer}} \xi_1 \to \cdots \to \xi_{N_{\mathrm{LF}}} = \xi' := (x'', v'') \tag{17}$$

   - Metropolis-Hastings accept / reject:

$$A(\xi'|\xi) = \min\left\{1, \frac{\pi(\xi')}{\pi(\xi)} \left|\mathcal{J}(\xi', \xi)\right|\right\}, \tag{18}$$

   where $|\mathcal{J}(\xi', \xi)|$ is the determinant of the Jacobian.

3. `backward:` (if training)

- Evaluate the loss function $\mathcal{L}(\xi', \xi)$ and back propagate

4. `return:` x_{i+1}

- Evaluate MH criteria (Eq. 18) and return accepted config:

$$x_{i+1} \leftarrow \begin{cases} x'' & \text{w/ prob.} \quad A(\xi'|\xi) \\ x & \text{w/ prob.} \quad 1 - A(\xi'|\xi) \end{cases} \tag{19}$$

3. Lattice Gauge Theories

3.1 2D $U(1)$ Model

We build upon the approach originally introduced in [17], which was successfully applied to the 2D $U(1)$ lattice gauge model in [8–10]. In particular, we are interested in measuring the (scalar) topological charge $Q \in \mathbb{Z}$ on the lattice. Since different lattice configurations with the same value of Q are related by a gauge transformation, they do not meaningfully contribute to our statistics.
Because of this, we would like to generate configurations from different *topological sectors* (characterized by different values of Q) to reduce uncertainty in our statistical estimates. By repeating this procedure at increasing spatial resolution[2] ($\beta \propto 1/a$), we are able to extrapolate our estimates to the continuum limit where they can be compared with experimental measurements. Current approaches such as HMC are known to suffer from auto-correlation times which scale exponentially in this limit, significantly limiting their effectiveness. This phenomenon can be seen in Fig 3, where fluctuations in the topological charge between sequential configurations (the *tunneling rate*) $\delta Q = |Q^{i+1} - Q^i|$ decreases as $\beta = 2 \to 3 \to \cdots$, and disappear completely (Q = const.) by $\beta = 7$.

Figure 3: $\delta Q \to 0$ with increasing β for the 2D $U(1)$ model. Image from [9].

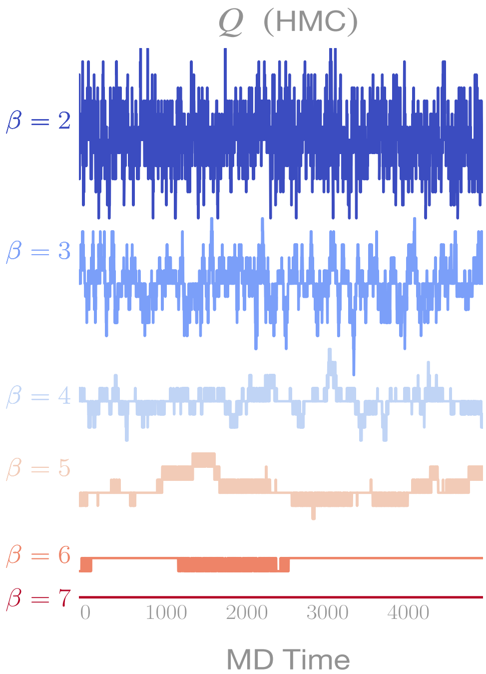

3.1.1 Results

Results for the 2D $U(1)$ model trained at $\beta = 4$ in $\simeq 25$ minutes on a single NVIDIA A100 GPU, using `l2hmc-qcd`. We provide the full Jupyter notebook containing the results in Fig 4.

3.2 4D $SU(3)$ Model

We would like to generalize this approach to handle 4D $SU(3)$ link variables $U_\mu(n) \in SU(3)$:

$$U_\mu(n) = \exp\left[i\omega^k_\mu(n)\lambda^k\right] \tag{20}$$

[2] Here a is the lattice spacing.

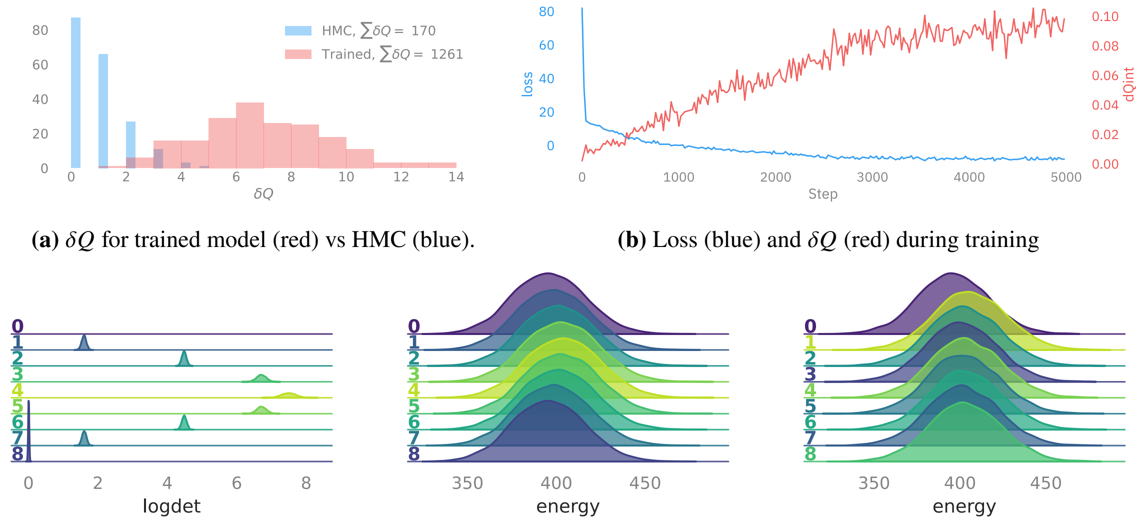

(a) δQ for trained model (red) vs HMC (blue). **(b)** Loss (blue) and δQ (red) during training

(c) $|\mathcal{J}|$ vs LF step *(trained)* **(d)** H vs LF step *(trained)* **(e)** H vs LF step *(HMC)*

Figure 4: Results from trained 2D $U(1)$ model at $\beta = 4$. In 4d we see the energy H increasing towards the middle of the trajectory, resulting in improved tunneling rate (larger δQ) in 4a. Jupyter notebook.

where $\omega^k_\mu(n) \in \mathbb{R}$ and λ^k are the generators of $SU(3)$. We consider the standard Wilson gauge action

$$S_G = -\frac{\beta}{6}\sum \mathrm{Tr}\left[U_{\mu\nu}(n) + U^\dagger_{\mu\nu}(n)\right], \quad \text{where} \tag{21}$$

$$U_{\mu\nu}(n) = U_\mu(n)U_\nu(n+\hat{\mu})U^\dagger_\mu(n+\hat{\nu})U^\dagger_\nu(n). \tag{22}$$

3.2.1 Generic MD Updates

As before, we introduce momenta $P_\mu(n) = P^k_\mu(n)\lambda^k$ conjugate to the real fields $\omega^k_\mu(n)$. We can write the Hamiltonian as

$$H[P,U] = \frac{1}{2}P^2 + S_G[U] \implies \boxed{\frac{d\omega^k}{dt} = \frac{\partial H}{\partial P^k}}, \quad \boxed{\frac{dP^k}{dt} = -\frac{\partial H}{\partial \omega^k}}. \tag{23}$$

To update the gauge field $U_\mu = e^{i\omega^k_\mu \lambda^k}$, write $\boxed{\frac{d\omega^k}{dt}\lambda^k = P^k\lambda^k}$ and discretize with step size ε:

$$-i\log U(\varepsilon) = -i\log U(0) + \varepsilon P(0) \tag{24}$$

$$U(\varepsilon) = e^{i\varepsilon P(0)}U(0) \implies \tag{25}$$

$$\boxed{\Lambda : U \longrightarrow U'} = e^{i\varepsilon P}U. \tag{26}$$

Similarly for the momentum update $\boxed{\frac{dP^k}{dt} = -\frac{\partial H}{\partial \omega^k}}$,

$$P(\varepsilon) = P(0) - \varepsilon F[U] \tag{27}$$

$$\boxed{\Gamma : P \longrightarrow P'} = P - \frac{\varepsilon}{2}F[U] \tag{28}$$

where $F[U]$ is the force term (see A.1).

3.2.2 Generalized MD Update

As in Sec.2, we introduce `pNet`: $(U, F) \longrightarrow (\alpha_P, \beta_P, \gamma_P)$ and `uNet`: $(U, P) \longrightarrow (\,\cdot\,, \beta_U, \gamma_U)$. Note that we have omitted the U scaling term (α_U) term in this update since $U \in SU(3)$. In terms of the generalized update operators,

$$\boxed{\Gamma_\theta^\pm} : (U, P) \xrightarrow{(\alpha_P, \beta_P, \gamma_P)} (U, P') \tag{29}$$

$$\boxed{\Lambda_\theta^\pm} : (U, P) \xrightarrow{(\,\cdot\,, \beta_U, \gamma_U)} (U', P) \tag{30}$$

we can write the complete update:

$$P' = \Gamma_\theta^\pm(U, P) \tag{31}$$

$$U' = U_B + \Lambda_\theta^\pm(U_A, P') \tag{32}$$

$$U'' = U'_A + \Lambda_\theta^\pm(U'_B, P') \tag{33}$$

$$P'' = \Gamma_\theta^\pm(U'', P') \tag{34}$$

Momentum Update
In this case, our `pNet` : $(U, F) = (\alpha_P, \beta_P, \gamma_P)$. We can write the generalized momentum update as $P^\pm := \Gamma_\theta^\pm(U, P)$, where[3]:

1. `forward`, $(+)$:

$$P^+ := \Gamma_\theta^+(U, P) = P \cdot e^{\frac{\varepsilon}{2}\alpha_P} - \frac{\varepsilon}{2}\left[F \cdot e^{\varepsilon\beta_P} + \gamma_P\right] \tag{35}$$

2. `backward`, $(-)$:

$$P^- := \Gamma_\theta^-(U, P) = e^{-\frac{\varepsilon}{2}\alpha_P} \cdot \left\{P + \frac{\varepsilon}{2}\left[F \cdot e^{\varepsilon\beta_P} + \gamma_P\right]\right\}. \tag{36}$$

By introducing the above modifications, we incur a factor of $\log\left|\frac{\partial P^\pm}{\partial P}\right| = \pm\frac{\varepsilon}{2}\sum \alpha_P$ in the Metropolis Hastings accept / reject $A(U'|U)$, and the sum is taken over the full trajectory.
Link Update
Similarly to the momentum update, the outputs from our `uNet` : $(U, P) \longrightarrow (\,\cdot\,, \beta_U, \gamma_U)$ are used in the generalized link update $U^\pm := \Lambda_\theta^\pm(U, P) = e^{i\varepsilon\tilde{P}^\pm}U$ (where $\tilde{P}^\pm \in \mathfrak{su}(3)$). Explicitly:

1. `forward`, $(+)$:

$$U^+ := \Lambda_\theta^+(U, P) = e^{i\varepsilon\tilde{P}^+}U, \quad \text{with} \quad \tilde{P}^+ = \left[P \cdot e^{\varepsilon\beta_U} + \gamma_U\right] \tag{37}$$

2. `backward`, $(-)$:

$$U^- := \Lambda_\theta^-(U, P) = e^{i\varepsilon\tilde{P}^-}U, \quad \text{with} \quad \tilde{P}^- = e^{-\varepsilon\beta_U} \cdot [P - \gamma_U] \tag{38}$$

[3]Note that $\left(\Gamma^+\right)^{-1} = \Gamma^-$, i.e. $\Gamma^+\left[\Gamma^-(U, F)\right] = \Gamma^-\left[\Gamma^+(U, F)\right] = (U, F)$, and similarly for $\Lambda^\pm$

3.3 Training

We construct a loss function using the expected squared charge difference

$$\mathcal{L}_\theta(U, U') = \mathbb{E}\left[A(U'|U) \cdot \delta_Q^2(U, U')\right], \tag{39}$$

where $\delta_Q^2(U, U') = |Q' - Q|^2$ is the squared topological charge (see A.2) difference between the initial and proposal configurations.

3.4 Results

For the trained 2D $U(1)$ model (Fig 4), we see in Fig 4c that $|\mathcal{J}|$ increases towards the middle of the trajectory, allowing for the sampler to overcome the large energy barriers between different topological sectors. This results in a greater *tunneling rate* (δQ) when compared to generic HMC. Identical behavior is observed after a short training run for the 4D $SU(3)$ model, as shown in Fig 5.

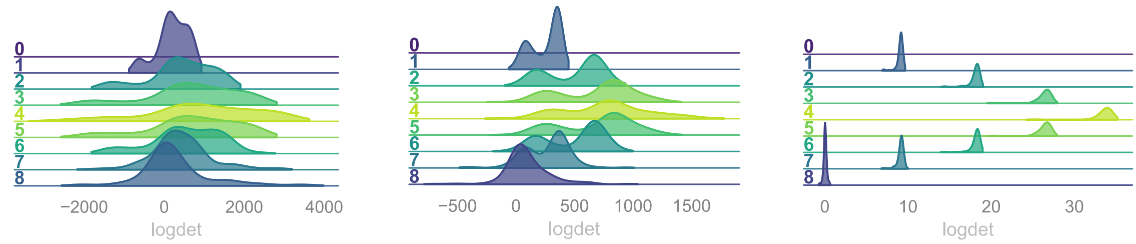

(a) 100 train steps **(b)** 500 train steps **(c)** 1000 train steps

Figure 5: Evolution of $|\mathcal{J}|$ during the first 1000 training iterations for the 4D $SU(3)$ model.

4. Conclusion

In this work we've introduced a generalized MD update for generating 4D $SU(3)$ gauge configurations that can be trained to improve sampling efficiency. Note that this is a relatively simple proof of concept demonstrating how to construct such a sampler. In a future work we plan to further investigate (and quantify) the cost / benefit when compared to alternative approaches such as traditional HMC and purely generative (OT / KL-Divergence [2–4, 15]) based approaches.

5. Acknowledgements

This research used resources of the Argonne Leadership Computing Facility, which is a DOE Office of Science User Facility supported under Contract DE-AC02-06CH11357. This research was supported by the Exascale Computing Project (17-SC-20-SC), a collaborative effort of the U.S. Department of Energy Office of Science and the National Nuclear Security Administration.

References

[1] M. Abadi, A. Agarwal, P. Barham, E. Brevdo, Z. Chen, C. Citro, G. S. Corrado, A. Davis, J. Dean, M. Devin, S. Ghemawat, I. Goodfellow, A. Harp, G. Irving, M. Isard, Y. Jia, R. Jozefowicz, L. Kaiser, M. Kudlur, J. Levenberg, D. Mane, R. Monga, S. Moore, D. Murray, C. Olah, M. Schuster, J. Shlens, B. Steiner, I. Sutskever, K. Talwar, P. Tucker, V. Vanhoucke, V. Vasudevan, F. Viegas, O. Vinyals, P. Warden, M. Wattenberg, M. Wicke, Y. Yu, and X. Zheng. TensorFlow: Large-scale machine learning on heterogeneous distributed systems. URL http://arxiv.org/abs/1603.04467.

[2] M. Albergo, G. Kanwar, and P. Shanahan. Flow-based generative models for markov chain monte carlo in lattice field theory. 100(3):034515, . ISSN 2470-0010, 2470-0029. doi: 10.1103/PhysRevD.100.034515. URL https://link.aps.org/doi/10.1103/PhysRevD.100.034515.

[3] M. S. Albergo, D. Boyda, D. C. Hackett, G. Kanwar, K. Cranmer, S. Racanière, D. J. Rezende, and P. E. Shanahan. Introduction to normalizing flows for lattice field theory, . URL http://arxiv.org/abs/2101.08176.

[4] D. Boyda, G. Kanwar, S. Racanière, D. J. Rezende, M. S. Albergo, K. Cranmer, D. C. Hackett, and P. E. Shanahan. Sampling using \$SU(n)\$ gauge equivariant flows. 103 (7):074504. ISSN 2470-0010, 2470-0029. doi: 10.1103/PhysRevD.103.074504. URL http://arxiv.org/abs/2008.05456.

[5] G. Cossu, P. Boyle, N. Christ, C. Jung, A. Jüttner, and F. Sanfilippo. Testing algorithms for critical slowing down. 175:02008. ISSN 2100-014X. doi: 10.1051/epjconf/201817502008. URL http://arxiv.org/abs/1710.07036.

[6] L. Dinh, J. Sohl-Dickstein, and S. Bengio. Density estimation using real NVP. URL http://arxiv.org/abs/1605.08803.

[7] M. Favoni, A. Ipp, D. I. Müller, and D. Schuh. Lattice gauge equivariant convolutional neural networks. 128(3):032003. ISSN 0031-9007, 1079-7114. doi: 10.1103/PhysRevLett.128.032003. URL http://arxiv.org/abs/2012.12901.

[8] S. Foreman, X.-Y. Jin, and J. C. Osborn. Deep learning hamiltonian monte carlo, . URL http://arxiv.org/abs/2105.03418.

[9] S. Foreman, X.-Y. Jin, and J. C. Osborn. LeapfrogLayers: A trainable framework for effective topological sampling, . URL http://arxiv.org/abs/2112.01582.

[10] S. A. Foreman. Learning better physics: a machine learning approach to lattice gauge theory. URL https://iro.uiowa.edu/esploro/outputs/doctoral/9983776792002771.

[11] A. Gelman and C. Pasarica. Adaptively scaling the metropolis algorithm using expected squared jumped distance. ISSN 1556-5068. doi: 10.2139/ssrn.1010403. URL http://www.ssrn.com/abstract=1010403.

[12] W. K. Hastings. Monte carlo sampling methods using markov chains and their applications. 57(1):97–109. ISSN 1464-3510, 0006-3444. doi: 10.1093/biomet/57.1.97. URL https://academic.oup.com/biomet/article/57/1/97/284580.

[13] M. Hoffman, P. Sountsov, J. V. Dillon, I. Langmore, D. Tran, and S. Vasudevan. NeuTra-lizing bad geometry in hamiltonian monte carlo using neural transport. URL http://arxiv.org/abs/1903.03704.

[14] J. D. Hunter. Matplotlib: A 2d graphics environment. 9(3):90–95. ISSN 1521-9615. doi: 10.1109/MCSE.2007.55. URL http://ieeexplore.ieee.org/document/4160265/.

[15] G. Kanwar, M. S. Albergo, D. Boyda, K. Cranmer, D. C. Hackett, S. Racanière, D. J. Rezende, and P. E. Shanahan. Equivariant flow-based sampling for lattice gauge theory. 125(12):121601. ISSN 0031-9007, 1079-7114. doi: 10.1103/PhysRevLett.125.121601. URL https://link.aps.org/doi/10.1103/PhysRevLett.125.121601.

[16] R. Kumar, C. Carroll, A. Hartikainen, and O. Martin. ArviZ a unified library for exploratory analysis of bayesian models in python. 4(33):1143. ISSN 2475-9066. doi: 10.21105/joss.01143. URL http://joss.theoj.org/papers/10.21105/joss.01143.

[17] D. Levy, M. D. Hoffman, and J. Sohl-Dickstein. Generalizing hamiltonian monte carlo with neural networks. URL http://arxiv.org/abs/1711.09268.

[18] Z. Li, Y. Chen, and F. T. Sommer. A neural network MCMC sampler that maximizes proposal entropy. URL http://arxiv.org/abs/2010.03587.

[19] M. Medvidovic, J. Carrasquilla, L. E. Hayward, and B. Kulchytskyy. Generative models for sampling of lattice field theories. URL http://arxiv.org/abs/2012.01442.

[20] Y. Nagai and A. Tomiya. Gauge covariant neural network for 4 dimensional non-abelian gauge theory. URL http://arxiv.org/abs/2103.11965.

[21] K. Neklyudov and M. Welling. Orbital MCMC. URL http://arxiv.org/abs/2010.08047.

[22] K. Neklyudov, M. Welling, E. Egorov, and D. Vetrov. Involutive MCMC: a unifying framework. URL http://arxiv.org/abs/2006.16653.

[23] F. Perez and B. E. Granger. IPython: A system for interactive scientific computing. 9(3): 21–29. ISSN 1521-9615. doi: 10.1109/MCSE.2007.53. URL http://ieeexplore.ieee.org/document/4160251/.

[24] D. J. Rezende, G. Papamakarios, S. Racanière, M. S. Albergo, G. Kanwar, P. E. Shanahan, and K. Cranmer. Normalizing flows on tori and spheres. URL http://arxiv.org/abs/2002.02428.

[25] C. P. Robert. The metropolis-hastings algorithm. URL http://arxiv.org/abs/1504.01896.

PoS(LATTICE2023)036

[26] S. Schaefer, R. Sommer, and F. Virotta. Investigating the critical slowing down of QCD simulations. In *Proceedings of The XXVII International Symposium on Lattice Field Theory — PoS(LAT2009)*, page 032. Sissa Medialab. doi: 10.22323/1.091.0032. URL https://pos.sissa.it/091/032.

[27] A. Sergeev and M. Del Balso. Horovod: fast and easy distributed deep learning in TensorFlow. URL http://arxiv.org/abs/1802.05799.

[28] A. Tanaka and A. Tomiya. Towards reduction of autocorrelation in HMC by machine learning. URL http://arxiv.org/abs/1712.03893.

[29] M. Waskom, O. Botvinnik, D. O'Kane, P. Hobson, S. Lukauskas, D. C. Gemperline, T. Augspurger, Y. Halchenko, J. B. Cole, J. Warmenhoven, J. De Ruiter, C. Pye, S. Hoyer, J. Vanderplas, S. Villalba, G. Kunter, E. Quintero, P. Bachant, M. Martin, K. Meyer, A. Miles, Y. Ram, T. Yarkoni, M. L. Williams, C. Evans, C. Fitzgerald, Brian, C. Fonnesbeck, A. Lee, and A. Qalieh. mwaskom/seaborn: v0.8.1 (september 2017). URL https://zenodo.org/record/883859.

[30] A. Wehenkel and G. Louppe. You say normalizing flows i see bayesian networks. URL http://arxiv.org/abs/2006.00866.

A. Appendix

A.1 Force Term

We can write the force term as

$$F = -\frac{1}{\lambda^2}\sum_k \lambda^k \operatorname{Tr}\left[i\left(UA - A^\dagger U^\dagger\right)\lambda^k\right] \tag{40}$$

where A is the sum over staples

$$A = \sum_{\mu\neq\nu} U_\mu(x+\hat{\mu})\, U_\mu^\dagger(x+\hat{\nu})\, U_\nu^\dagger(x) \tag{41}$$

$$+ \sum_{\mu\neq\nu} U_{-\nu}(x+\hat{\mu})\, U_\mu^\dagger(x-\hat{\nu})\, U_{-\nu}^\dagger(x). \tag{42}$$

Since, $i\left(UA - A^\dagger U^\dagger\right) \in \mathfrak{su}(3)$, we can write it in terms of the generators λ^k as

$$\sum_k \lambda^k \operatorname{Tr}\left[\lambda^k \sum_j c_j\, \lambda^j\right] = \sum_k \sum_j c_j\, \lambda^j \operatorname{Tr}\left[\lambda^k \lambda^j\right] \tag{43}$$

$$= \frac{1}{2}\sum_k \sum_j c_j\, t^k\, \delta_{jk} \tag{44}$$

$$= \frac{1}{2}\sum_k c_k\, t^k \tag{45}$$

consequently, we can simplify the force term as

$$F[U] = -\frac{1}{2g^2}\, i\left(UA - A^\dagger U^\dagger\right). \tag{46}$$

A.2 Topological Charge Q

In lattice field theory, the topological charge Q is defined as the 4D integral over spacetime of the topological charge density q. In the continuum,

$$Q = \int d^4 x q(x), \text{ where} \tag{47}$$

$$q(x) = \frac{1}{32\pi^2}\epsilon_{\mu\nu\rho\lambda}\mathrm{Tr}\left\{F_{\mu\nu}F_{\rho\lambda}\right\} \tag{48}$$

On the lattice, we choose a discretization[4] $q_L(x)$ such that $Q = a^4 \sum_x q_L(x)$. The most obvious discretization of q_L uses the 1×1 plaquette $P_{\mu\nu}(x)$, and can be written as

$$q_L^{\text{plaq}}(x) = \frac{1}{32\pi^2}\epsilon_{\mu\nu\rho\lambda}\mathrm{Tr}\left\{P_{\mu\nu}(x)P_{\rho\lambda}(x)\right\} \tag{49}$$

this has the advantage of being computationally inexpensive, but leads to lattice artifacts of order $O(a^2)$.

[4]We are free to choose a specific discretization as long as it gives the right continuum limit